J|A|C|S
ARTICLES
Published on Web 09/25/2004

Metal-Catalyzed Anaerobic Disproportionation of Hydroxylamine. Role of Diazene and Nitroxyl Intermediates in the Formation of N_2, N_2O, NO^+, and NH_3

Graciela E. Alluisetti,[†] Alejandra E. Almaraz,[†] Valentín T. Amorebieta,*[,†] Fabio Doctorovich,[‡] and José A. Olabe*[,‡]

Contribution from the Departamento de Química, Facultad de Ciencias Exactas, Universidad Nacional de Mar del Plata, Funes y R. Peña, Mar del Plata B7602AYL, Argentina, and Departamento de Química Inorgánica, Analítica y Química Física, INQUIMAE, Facultad de Ciencias Exactas y Naturales, Universidad de Buenos Aires, Pabellón 2, Ciudad Universitaria, Buenos Aires C1428EHA, Argentina

Received June 3, 2004; E-mail: amorebie@mdp.edu.ar; olabe@qi.fcen.uba.ar

Abstract: The catalytic disproportionation of NH_2OH has been studied in anaerobic aqueous solution, pH 6−9.3, at 25.0 °C, with $Na_3[Fe(CN)_5NH_3]\cdot 3H_2O$ as a precursor of the catalyst, $[Fe^{II}(CN)_5H_2O]^{3-}$. The oxidation products are N_2, N_2O, and NO^+ (bound in the nitroprusside ion, NP), and NH_3 is the reduction product. The yields of N_2/N_2O increase with pH and with the concentration of NH_2OH. *Fast regime* conditions involve a chain process initiated by the NH_2 radical, generated upon coordination of NH_2OH to $[Fe^{II}(CN)_5H_2O]^{3-}$. NH_3 and nitroxyl, HNO, are formed in this fast process, and HNO leads to the production of N_2, N_2O, and NP. An intermediate absorbing at 440 nm is always observed, whose formation and decay depend on the medium conditions. It was identified by UV−vis, RR, and ^{15}NMR spectroscopies as the diazene-bound $[Fe^{II}(CN)_5N_2H_2]^{3-}$ ion and is formed in a competitive process with the radical path, still under the fast regime. At high pH's or NH_2OH concentrations, an *inhibited regime* is reached, with slow production of *only* N_2 and NH_3. The stable red diazene-bridged $[(NC)_5FeHN{=}NHFe(CN)_5]^{6-}$ ion is formed at an advanced degree of NH_2OH consumption.

Introduction

Hydroxylamine (NH_2OH) is important in the synthesis of caprolactam, a precursor of polyamide 6, and is also employed as a reducing agent for photographic processes and dyeing and in the production of oximes for use in paints, pharmaceuticals, and pesticides.[1] It is formed as an intermediate during the reversible bacterial interconversions of ammonia into nitrite and/or nitrate in aerobic soils.[2] Nitrosomonas europaea derives energy for growth from the oxidation of ammonia to nitrite. Two enzymes are involved: ammonia monooxygenase, a membrane-bound enzyme that catalyses the oxidation of ammonia in the reaction $NH_3 + O_2 + 2e^- + 2H^+ \rightarrow NH_2OH + H_2O$, and hydroxylamine oxidoreductase (HAO), a soluble multiheme enzyme that catalyzes the reaction: $NH_2OH + H_2O \rightarrow NO_2^- + 4e^- + 5H^+$.[3,4] NH_2OH can be reduced to NH_3 by some heme cd_1−[5a,b] and cytochrome *c*-containing nitrite reductases (NiR),[5c,d] as well as by some sulfite reductases.[5e,f] NH_2OH is a natural product of mammalian cells and is produced through the decomposition of nitrosothiols.[6] It is widely used as an NO donor;[7] thus, although it inhibits guanylate cyclase activity, a vasorelaxing activation is obtained in the presence of catalase-H_2O_2.[6] Reactions with oxyhemoglobin and myoglobin are also considered biochemically significant.[6,7]

In the reactions with transition metal complexes, NH_2OH behaves as a strong reductant, leading to diverse oxidized products or as an oxidizing agent producing ammonia, depending on the metal and spectator ligands, the pH, and the medium.[8] Free radicals derived from one-electron reduction or oxidation of NH_2OH (NH_2 or NHOH, respectively) have been detected as intermediates in some of these reactions.[8]

[†] Universidad Nacional de Mar del Plata.
[‡] Universidad de Buenos Aires.

(1) Buchner, W.; Schliebs, R.; Winter, O.; Buchel, K. H. *Industrial Inorganic Chemistry*; VCH Veriagsgeselischaft: 1989; pp 52−55.
(2) Hughes, M. N. *The Inorganic Chemistry of Biological Processes*, 2nd ed; Wiley: New York, 1981.
(3) Hooper, A. B. In *Autotrophic Bacteria*; Schlegel, H. G., Bowien, B., Eds.; Science Tech Publishers: 1989.
(4) (a) Hendrich, M. P.; Logan, M.; Andersson, K. K.; Arciero, D. M.; Lipscomb, J. D.; Hooper, A. B. *J. Am. Chem. Soc*. **1994**, *116*, 11961−11968. (b) Hendrich, M. P.; Petasis, D.; Arciero, D. M.; Hooper, A. B. *J. Am. Chem. Soc*. **2001**, *123*, 2997−3005. (c) Upadhyay, A. K.; Petasis, D. T.; Arciero, D. M.; Hooper, A. B.; Hendrich, M. P. *J. Am. Chem. Soc*. **2003**, *125*, 1738−1747. (d) Hendrich, M. P.; Upadhyay, A. K.; Riga, J.; Arciero, D. M.; Hooper, A. B. *Biochemistry* **2002**, *41*, 4603−4611. (e) Cabail, M. Z.; Pacheco, A. A. *Inorg. Chem*. **2003**, *42*, 270−272.
(5) (a) Allen, J. W. A.; Watmough, N. J.; Ferguson, S. J. *Nat. Struct. Biol*. **2000**, *7*, 885−888. (b) Singh, J. *Biochim. Biophys. Acta* **1973**, *333*, 28−36. (c) Stach, P.; Einsle, O.; Schumacher, W.; Kurun, E.; Kroneck, P. M. H. *J. Inorg. Biochem*. **2000**, *79*, 381−385. (d) Einsle, O.; Messerschmidt, A.; Huber, R.; Kroneck, P. M. H.; Neese, F. *J. Am. Chem. Soc*. **2002**, *124*, 11737−11745. (e) Lui, S. M.; Soriano, A.; Cowan, J. A. *J. Am. Chem. Soc*. **1993**, *115*, 10483−10486. (f) Crane, B. R.; Siegel, L. M.; Getzoff, E. D. *Biochemistry* **1997**, *36*, 12120−12137.
(6) Feelisch, M.; Stamler, J. S., Eds. *Methods in Nitric Oxide Research*; Wiley: Chichester, 1996.
(7) Wang, P. G.; Xian, M.; Tang, X.; Wu, X.; Wen, Z.; Cai, T.; Janczuk, A. J. *Chem. Rev*. **2002**, *102*, 1091−1134.
(8) Wieghardt, K. *Adv. Inorg. Bioinorg. Mech.* **1984**, *3*, 213−274.

10.1021/ja046724i CCC: $27.50

Slow disproportionation of NH_2OH in alkaline solutions gives NH_3 and N_2/N_2O mixtures.[9] These processes are also apparent in the reactions of NH_2OH with iron porphyrins and bacteria.[5f,10] It has been suggested that this reaction type only occurs in the presence of metal ion catalysts, involving coordination of NH_2-OH to the metal.[11] In general, the redox properties of coordinated NH_2OH as compared to the free ligand have not been studied in great detail.[8]

We focus on the reactivity of NH_2OH bound to the $[Fe^{II}(CN)_5]^{3-}$ fragment.[12] The pentacyano(L)ferrate(II) complexes are well characterized systems, and many L ligands form moderate to strong stable complexes (K_{st} = ca. 10^3-10^5 M^{-1}). In many cases, the pentacyano(L)ferrate(III) derivatives have been also characterized.[13] The potential for the Fe(III),Fe(II) couple to catalyze ligand redox is intriguing. Reactive intermediates may be stabilized by the $[Fe^{II}(CN)_5]^{3-}$ fragment during these redox processes.[14] The catalytic disproportionation of NH_2-OH using nitroprusside (NP) has been considered,[15,16] but the mechanistic proposal admits a significant revision, as will be shown here. Our main goal is to investigate the mechanism of the catalytic disproportionation reaction(s) of NH_2OH in anaerobic medium, with an eye toward characterizing its coordination ability to the iron center. We address the conditions favoring the formation of N_2 vs N_2O and NO^+/NO_2^-.

Experimental Section

Reagents. $Na_3[Fe(CN)_5NH_3]\cdot 3H_2O$ was synthesized and purified according to literature procedures.[17] $NH_2OH\cdot HCl$ (Merck, 99%), $^{15}NH_2$-$OH\cdot HCl$ (Isotec, 99% of ^{15}N atoms), $(N_2H_5)_2SO_4$, pyrazinamide, D_2O, 95% thiosuccinic acid, and 99% methyl methacrylate (Aldrich) were used as received. N_2 and Ar (AGA, UAP) were used for previous bubbling of the solutions. The buffer solutions were prepared using reagent grade $Na_2B_4O_7\cdot 10H_2O$ (Merck, 99%), KH_2PO_4 (Merck, 99%), and NaOH (Anwill, 99%). Deionized distilled water was used in all the experiments.

Physical Measurements. UV−vis spectra were recorded in a UV 2101-PC Shimadzu instrument, in the range 300−900 nm. Complementary measurements in the near-infrared region (NIR), up to 1500 nm, were obtained with a Shimadzu 3101 PC instrument. Some kinetic runs were carried out with an Applied Photophysics RX 1000 stopped flow (SF) accessory, linked to a Hewlett-Packard 8453 diode array spectrophotometer. Qualitative and quantitative gas production were conducted using a thermostated homemade flow reactor (volume, 0.07 dm^3) linked to a vacuum system and to an Extrel Emba II quadrupolar mass spectrometer through a thin thermostated capillary. The reactor was also supplied with an absolute pressure transducer, MKS Baratron 622 A, and with a mechanical stirrer. The pH was controlled with a Hanna HI9321 pHmeter, calibrated against Merck standard buffers. The NMR studies (^{15}N) were performed in a Bruker 500 MHz instrument, using Ar-flushed solutions of $Na_3[Fe(CN)_5NH_3]\cdot 3H_2O$ in D_2O (ca. 0.06 M, pH 9), after adding a great excess of $^{15}NH_2OH$. IR spectra were obtained using either a Thermo Mattson (model Genesis II) or a Nicolet 510P FTIR instrument. Resonance Raman spectra were measured with the 457.9-nm excitation line of an Ar^+-laser (Coherent Innova 400) using an U1000, ISA spectrograph equipped with a liquid nitrogen cooled CCD camera. The spectral resolution was 4 cm^{-1}, and the step width (increment per data point) was 0.53 cm^{-1}. Accumulation times of the spectra were 15 s. The samples were placed in a rotating cell to avoid photodamage by the incident beam (power of ca. 30 mW). Phenol was determined with a Konic HPLC instrument model KNK-500-A containing a UV−vis detector.

Procedures and Identification of Reactants and Products. At pH's 6−8, the dissociation of NH_3 from the $[Fe(CN)_5NH_3]^{3-}$ ion (λ_{max} = 396 nm, ϵ = 450 M^{-1} cm^{-1}) yields quantitatively the $[Fe(CN)_5H_2O]^{3-}$ ion in a few minutes (λ_{max} = 444 nm, ϵ = 660 M^{-1} cm^{-1}).[18] This species decays slowly through a decomposition process leading to the $[Fe(CN)_6]^{4-}$ and Fe^{2+} ions by way of successive release and recombination of cyanides ($t_{1/2}$ = ca. 2 h).[19] Thus, it is sufficiently long-lived, relative to the time scale of the main reactions under study, to trap the free ligands present in the solutions. We checked spectroscopically on these dissociation−decomposition processes, to put them under control in our reaction conditions, including the absence of perturbations associated with oxygen leakage. Due to the possible catalytic role of the ferrous ions, we verified that the distribution of products in the experiments to be described below did not change by adding a great excess of EDTA as a potential scavenger.[18,20]

The experiments were carried out under oxygen-free conditions (bubbling with, and mixed under N_2 or Ar), avoiding the formation of the $[Fe^{III}(CN)_5H_2O]^{2-}$ ion (λ_{max} = 394 nm, ϵ = 750 M^{-1} cm^{-1}),[21] potentially produced by oxidation of $[Fe^{II}(CN)_5H_2O]^{3-}$.[18]

The reactions were studied at 25.0 °C in buffer solution (0.1 or 1 M in phosphates for pH 6−8 or 0.1 M in Borax for pH 9.3). The detailed procedures were as follows. For the UV−vis kinetic experiments, $Na_3[Fe(CN)_5NH_3]\cdot 3H_2O$ was dissolved in a volume of buffer solution (final concentration $(0.02-3.0)\times 10^{-3}$ M). A sample was put in the quartz cell (optical path 0.1 or 1 cm) and a desired amount of NH_2OH solution was added over the range $2\times 10^{-5}-10^{-1}$ M. Absorbance values at fixed wavelengths (440, 520 nm) were registered as a function of time. The kinetic runs in the SF regime were performed under pseudo-first-order conditions in NH_2OH ($(2.0-5.0)\times 10^{-3}$ M, I = 1 M, NaCl; pH 7), by monitoring, at 440 nm, the decay of the absorbance of 1.0×10^{-4} M $[Fe(CN)_5H_2O]^{3-}$. The measured values were fitted to $\ln(A_t - A_\infty)$ against time. The pseudo-first-order rate constants (k_{obs}/s^{-1}) were plotted against $[NH_2OH]_0$, thus obtaining a second-order rate constant (k_f/M^{-1} s^{-1}). For the measurement of the gaseous products, 0.025−0.040 dm^3 of a buffered solution of NH_2OH at the desired concentration ($5\times 10^{-4} - 2\times 10^{-1}$ M) and a measured amount of solid $Na_3[Fe(CN)_5NH_3]\cdot 3H_2O$ (final concentration, $(1-3)\times 10^{-3}$ M) were placed separately inside the reactor. Both reactants were mixed after evacuation, and the time evolution of the gaseous stream was continuously monitored. The evolution of the total pressure of the system (p_{sys}) was obtained by numerical integration of the balance equation: $(dp_{sys}/dt) = (dp_{obs}/dt) + (k_e \times p_{obs}^2)$, with p_{obs} being the measured pressure and $k_e \approx 2\times 10^{-5}$ $Torr^{-1}$ min^{-1}, the leak constant. The products of the reaction were N_2 and N_2O, and quantitative determinations required the calibration of the mass spectrometer

(9) (a) Nast, R.; Hieber, W.; Proeschel, E. *Z. Anorg. Allg. Chem.* **1948**, *13*, 339. (b) Nast, R.; Foppel, J. *Z. Anorg. Allg. Chem.* **1950**, *263*, 310.
(10) (a) Choi, I. K.; Liu, Y.; Wei, Z.; Ryan, M. D. *Inorg. Chem.* **1997**, *36*, 3113−3118. (b) Barley, M. H.; Takeuchi, K. J.; Meyer, T. J. *J. Am. Chem. Soc.* **1986**, *108*, 5876−5885. (c) Bazylinski, D. A.; Arkowitz, R. A.; Hollocher, T. C. *Arch. Biochem. Biophys.* **1987**, *259*, 520−526. (d) Castignetti, D.; Hollocher, T. C. *Appl. Environm. Microbiol.* **1982**, *44*, 923−928. (e) Bagchi, S. N.; Kleiner, D. *Biochim. Biophys. Acta* **1990**, *1041*, 9−13.
(11) (a) Lunak, S.; Veprek-Siska, J. *Collect. Czech. Chem. Commun.* **1974**, *39*, 41−48. (b) Lunak, S.; Veprek-Siska, J. *Collect. Czech. Chem. Commun.* **1974**, *39*, 391−395. (c) Bonner, F. T.; Akhtar, M. J. *Inorg. Chem.* **1981**, *20*, 3155−3160.
(12) Lunak, S.; Veprek-Siska, J. *Collect. Czech. Chem. Commun.* **1974**, *39*, 2719−2723.
(13) (a) Macartney, D. H. *Rev. Inorg. Chem.* **1988**, *6*, 101−151. (b) Baraldo, L. M.; Forlano, P.; Parise, A. R.; Slep, L. D.; Olabe, J. A. *Coord. Chem. Rev.* **2001**, *219*−*221*, 881−921.
(14) Olabe, J. A. *Adv. Inorg. Chem.* **2004**, *55*, 61−126.
(15) Banyai, I.; Dozsa, L.; Beck, M. T.; Gyemant, G. *J. Coord. Chem.* **1996**, *37*, 257−270.
(16) Wolfe, S. K.; Andrade, C.; Swinehart, J. H. *Inorg. Chem.* **1974**, *13*, 2567−2572.
(17) Kenney, D. J.; Flynn, T. P.; Gallini, J. B. *J. Inorg. Nucl. Chem.* **1961**, *20*, 75−81.
(18) Toma, H. E. *Inorg. Chim. Acta* **1975**, *15*, 205−211.
(19) Olabe, J. A.; Zerga, H. O. *Inorg. Chem.* **1983**, *22*, 4156−4158.
(20) Bridgart, G. J.; Waters, W. A.; Wilson, I. R. *J. Chem. Soc., Dalton Trans.* **1973**, 1582−1584.
(21) Espenson, J. H.; Wolenuk, S. G., Jr. *Inorg. Chem.* **1972**, *11*, 2034−2041.

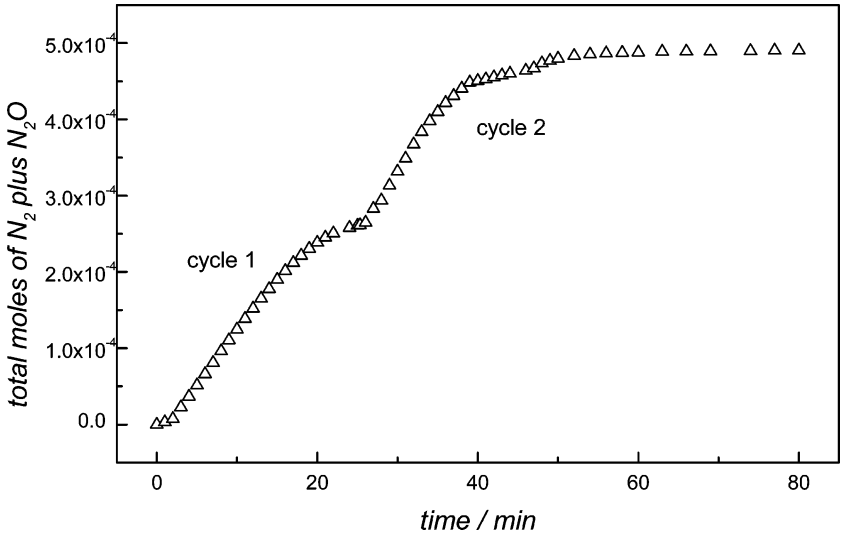

Figure 1. Time evolution of the total gaseous products (in moles) during the successive addition of 5×10^{-2} M NH_2OH ($R_0 = 20$) over 2.5×10^{-3} M $[Fe(CN)_5H_2O]^{3-}$ (0.025 dm^3 of buffer solution), at pH 8, $I = 2.6$ M (phosphates), 25 °C.

sensibilities. The solubility of N_2O in the buffer solutions was considered by measuring independently its Henry constant. From the values of the calculated p_{sys} and the solubility of N_2O, a corrected molar fraction and the concentration of the gaseous products in the condensed phase were established. We verified that the redox capacity in the exhausted solutions was nearly equal to the one corresponding to the initial $[Fe^{II}(CN)_5NH_3]^{3-}$, by titration with iodine;[22] in this way, the absence of oxidized $[Fe^{III}(CN)_5L]^{n-}$ or reducing (NH_2OH, N_2H_4) species was confirmed. Ammonia, NP, and the $[(NC)_5FeN_2H_2Fe(CN)_5]^{6-}$ ion were identified and quantified in these solutions. Ammonia was extracted by distillation under N_2 current; it was identified by mass spectrometry and quantified by acid/base titration. Alternatively, a spectral quantification was made directly on the residual solutions by means of its reaction product with a solution of phenol and hypochlorite ion containing NP as catalyst.[23] NP was identified in the solid residue by IR spectroscopy[24] and quantified in the solutions through the reaction with thiosuccinic acid.[25] It was also indirectly confirmed in the reacting solutions by means of the reaction with 1,2-dimethylhydrazine,[26] whose product led to a typical EPR signal of the $[Fe(CN)_5NO]^{3-}$ radical.[27] The $[(NC)_5FeN_2H_2Fe(CN)_5]^{6-}$ complex was identified in some of the exhausted solutions (pH 8−9.3, in assays performed with great excess of NH_2OH) by its absorption band at 520 nm, in agreement with a previous characterization based on gel-permeation experiments and RR measurements.[28] We report now that a product with the same absorption features has been obtained in an independent two-step experiment: first, a solution of the $[Fe(CN)_5N_2H_4]^{3-}$ ion[29] was titrated with 2 equiv of hexacyanoferrate(III), leading to a 440-nm absorbing product, $[Fe(CN)_5N_2H_2]^{3-}$ (see Results). This solution was mixed with an equivalent of $[Fe^{II}(CN)_5NH_3]^{3-}$, with the ensuing development of the 440-nm → 520-nm conversion. Control experiments showed that the decomposition of NH_2OH was very slow in the absence of $[Fe(CN)_5NH_3]^{3-}$, with an observed rate of formation of gaseous products lower than 10^{-6} M min^{-1}. This value is about 1 order of magnitude smaller than the slowest rate measured in the presence of complex.

Numerical simulations were performed by using a specific program, based on an adaptation of the "predictor−corrector" approach developed by Gear.[30]

Results

(i) Catalytic Behavior. When solutions of excess NH_2OH are mixed with $[Fe^{II}(CN)_5NH_3]^{3-}$, the evolution of N_2 and N_2O is rapidly observed, with formation of NH_3 in the residual solutions. Clearly, a disproportionation process is underway. For a constant concentration of complex, the catalytic behavior can be visualized by making successive additions of NH_2OH to the exhausted reaction mixtures. The parameter $R_0 = \{[NH_2OH]_0/[Fe(CN)_5NH_3{}^{3-}]_0\}$, where $[NH_2OH]_0$ and $[Fe(CN)_5NH_3{}^{3-}]_0$ are the initial concentrations, will be used further on. Figure 1 shows the time evolution of the number of moles of total gaseous products for $R_0 = 20$ and pH 8. After an induction period of a few minutes, a plateau region is attained in approximately 25 min, with total consumption of initial NH_2OH. If the same amount of NH_2OH is added again to the mixture, a fast response (i.e., without the induction period described above) is obtained, and the gas evolution proceeds with a similar rate profile as in the first cycle. The system evolves in the same catalytic way if previously oxidized $[Fe^{III}(CN)_5L]^{n-}$ (L = NH_3, H_2O) is added as a starter, instead of Fe(II). On the other hand, the catalytic process is not observed if $[Fe(CN)_6]^{4-}$ is initially used, or through the addition of L ligands forming very stable $[Fe^{II}(CN)_5L]^{n-}$ complexes, such as cyanide, pyrazinamide, and the like.[13] To confirm that the $[Fe(CN)_5]^{3-}$ fragment remains intact along the reaction, we carried out experiments with $^{15}NH_2OH$, which showed unequivocally only ^{15}N-containing products.

(ii) Stoichiometry. The balances of nitrogen were performed at iron concentrations of ca. 10^{-3} M. The transformed NH_2OH corresponds to: $n^0_{NH_2OH} \approx [(4 \times n_{N_2O} + 3 \times n_{N_2})]$ (see Table 1), where $n^0_{NH_2OH}$ is the number of initial moles of NH_2OH and n_{N_2O}, n_{N_2} are the moles of products at the end of the reaction. We estimate the errors in the nitrogen balances around 20%

(22) Siggia, S.; Hanna, J. G. *Quantitative Organic Analysis via Functional Groups*, 4th ed.; Wiley-Interscience: 1979.
(23) Koroleff, F. In *Methods of Seawater Analysis*; Grasshoftt, K., Ed.; Verlag Chemie: New York, 1976; pp 126−133.
(24) Paliani, G.; Poletti, A.; Santucci, A. *J. Mol. Struct.* **1971**, *8*, 63−74.
(25) Szacilowski, K.; Stochel, G.; Stasicka, Z.; Kisch, H. *New J. Chem*. **1997**, *21*, 893−902.
(26) Gutiérrez, M. M.; Amorebieta, V. T.; Estiú, G. L.; Olabe, J. A. *J. Am. Chem. Soc*. **2002**, *124*, 10307−10319.
(27) van Voorst, J. D. W.; Hemmerich, P. *J. Chem. Phys*. **1966**, *45*, 3914−3918.
(28) Funai, I. A.; Blesa, M. A.; Olabe, J. A. *Polyhedron* **1989**, *8*, 419−426.
(29) (a) Katz, N. E.; Olabe, J. A.; Aymonino, P. J. *J. Inorg. Nucl. Chem*. **1977**, *39*, 908−910. (b) Olabe, J. A.; Gentil, L. A. *Transition Met. Chem*. **1983**, *8*, 65−69.
(30) Gear, C. W. *Comun. ACM* **1971**, *14*, 176.

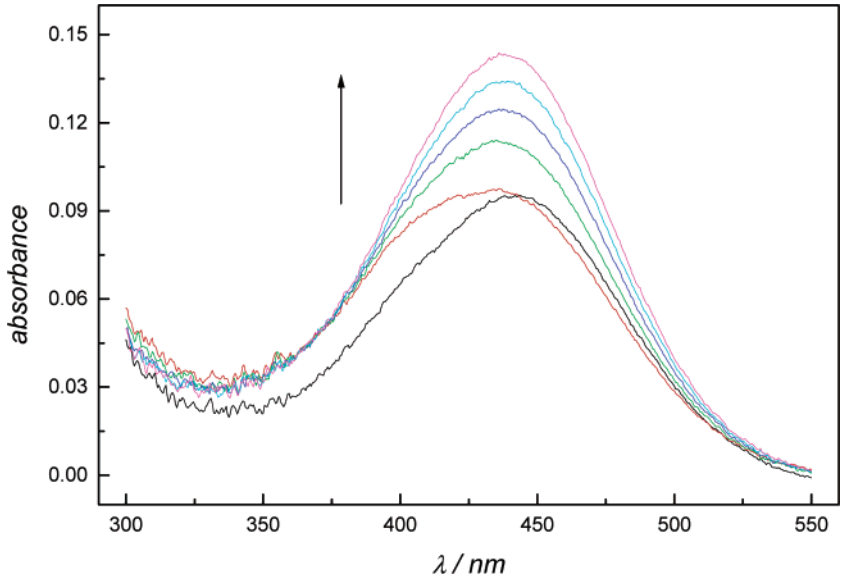

Figure 2. Successive spectra obtained during the reaction of 1.5×10^{-4} M $[Fe(CN)_5H_2O]^{3-}$ with 9×10^{-4} M NH_2OH ($R_0 = 6$), pH 7, $I = 1.9$ M (phosphates), 25.0 °C. Time elapsed between initial and final spectra: 5 min.

Table 1. Measured Values of N_2O and N_2 Concentrations Obtained in the Catalytic Decomposition Experiments, with Variation of pH and Concentration of Initial NH_2OH, at Constant Initial $[Fe(CN)_5NH_3]^{3-}$: $(2.0-2.5) \times 10^{-3}$ M

pH	$[NH_2OH]_0$[a]	R_0[b]	$[N_2O]$[c]	$[N_2]$[c]	$[N_2]/[N_2O]$[c]	%N yield[d]
7.0	1.25×10^{-2}	5	1.3×10^{-3}	2.3×10^{-3}	1.8	97
7.0	5.0×10^{-2}	20	4.6×10^{-3}	9.8×10^{-3}	2.1	96
7.0	7.5×10^{-2}	30	7.0×10^{-3}	1.5×10^{-2}	2.1	97
7.0	0.21	85	1.0×10^{-3}	7.2×10^{-2}	72.0	103
8.0	5.0×10^{-3}	2	8.3×10^{-4}	3.6×10^{-4}	0.4	88
8.0	1.25×10^{-2}	5	1.5×10^{-3}	2.3×10^{-3}	1.5	103
8.0	5.0×10^{-2}	20	5.6×10^{-3}	9.2×10^{-3}	1.6	100
8.0	7.5×10^{-2}	30	2.4×10^{-3}	2.0×10^{-2}	8.3	93
8.0	0.10	40	8.0×10^{-4}	3.1×10^{-2}	38.8	96
9.3	1.25×10^{-2}	5	2.6×10^{-3}	7.0×10^{-4}	0.3	100
9.3	5.0×10^{-2}	20	6.2×10^{-3}	8.2×10^{-3}	1.3	99
9.3	7.5×10^{-2}	30	7.0×10^{-4}	2.3×10^{-2}	32.9	95

[a] Molar concentration (M). [b] $R_0 = \{[NH_2OH]_0/[Fe(CN)_5NH_3^{3-}]_0\}$ [c] Molar concentration (M) expressed in the condensed phase. [d] Calculated using $\{[(4[N_2O] + 3[N_2])/[NH_2OH]_0]\} \times 100$.

when the reaction products are N_2, N_2O, NH_3, and NP and below 10% when N_2 and NH_3 are exclusively produced (see below for the two described regimes, fast and slow, respectively). The results indicate that the global operating processes for the gas evolution can be described by the following equations:

$$4NH_2OH \rightarrow N_2O + 2NH_3 + 3H_2O$$

$$3NH_2OH \rightarrow N_2 + NH_3 + 3H_2O$$

(iii) Spectroscopic and Kinetic Evidence for the Coordination of NH_2OH. Figure 2 shows the successive spectra of the solutions affording gas evolution and formation of NH_3, at pH 7. Although the initial 440-nm absorption of $[Fe(CN)_5H_2O]^{3-}$ shifts to lower wavelengths just after mixing, a new, more intense band develops, also at 440 nm, with increasing time. This behavior is also observed with ca. 10^{-3} M $[Fe(CN)_5H_2O]^{3-}$, maintaining $R_0 > 1$. The initial shift is indicative of NH_2OH coordination, as the time scale is consistent with the SF kinetic study of the primary interaction of $[Fe(CN)_5H_2O]^{3-}$ with excess NH_2OH, monitoring the decay of $[Fe(CN)_5H_2O]^{3-}$ at pH 7, for

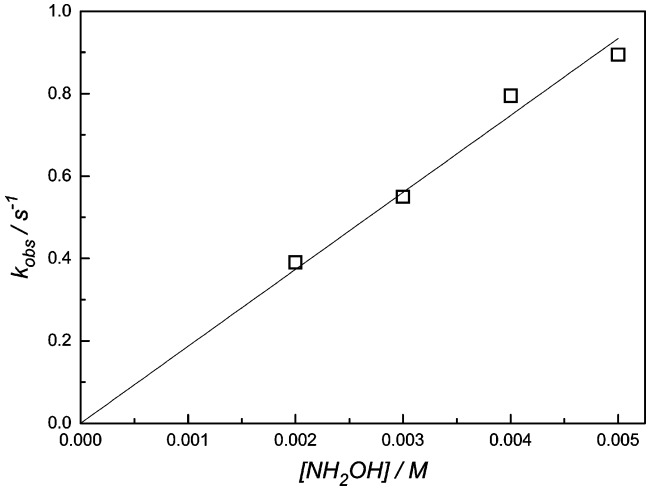

Figure 3. Plot of k_{obs} (s^{-1}) vs $[NH_2OH]$ in the reaction of 1.0×10^{-4} M $[Fe(CN)_5H_2O]^{3-}$, with a controlled excess of NH_2OH, $I = 1$ M, NaCl; pH 7 (phosphates), 25 °C.

short times. These results lead to well-behaved pseudo-first-order plots (Figure SI 1). Figure 3 displays a linear dependence of k_{obs} (s^{-1}) on $[NH_2OH]$, from which a value of $k_f = 190$ M^{-1} s^{-1} has been obtained. On the other hand, the intense 440-nm absorption observed for longer times in Figure 2 reflects the buildup of another intermediate, as shown below.

(iv) Evidence for Oxidation of Fe(II) to Fe(III) upon Coordination. The following results were obtained at comparable or slightly deficient concentrations of NH_2OH with respect to the iron complex, given that, in the presence of excess NH_2OH, the subsequent reactivity described above hides all evidence of the Fe(III) chromophore. Figure 4 shows the successive UV−vis spectra obtained after mixing equimolar solutions of $[Fe(CN)_5H_2O]^{3-}$ and NH_2OH, at pH 7.

The decay at 444 nm is accompanied by the onset of a band centered at 395 nm, with a similar intensity, along with a pronounced bending of the baseline for wavelengths above 700 nm. This corresponds to the tail of a new emerging broad band in the NIR region centered at ca. 1400 nm, corresponding to

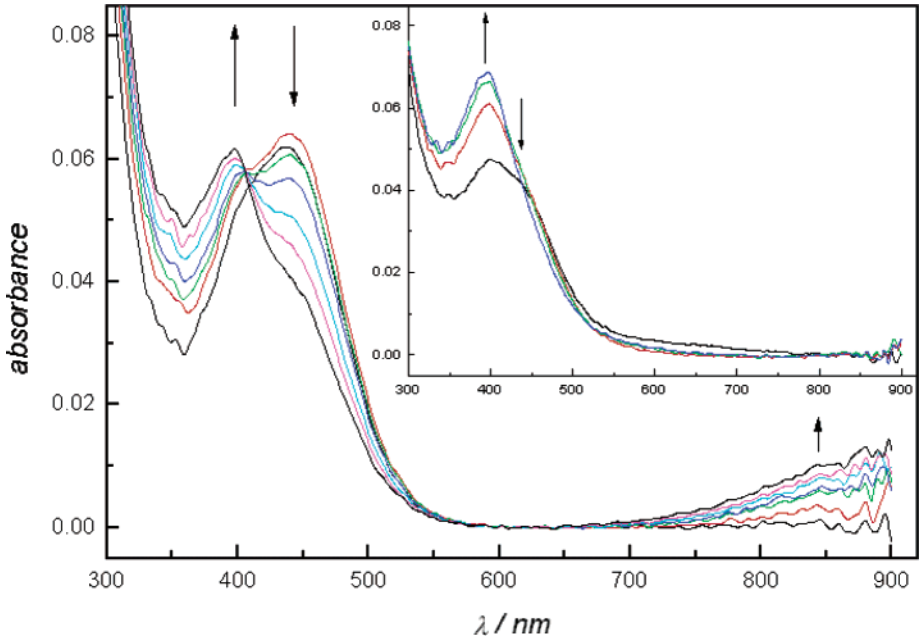

Figure 4. Successive UV−visible spectra obtained during the reaction of 8×10^{-5} M $[Fe(CN)_5H_2O]^{3-}$ with 8×10^{-5} M NH_2OH, pH 7, $I = 1.9$ M (phosphates), $T = 25$ °C. Inset: same as before, pH 9.3. The shoulder at 440 nm in the initial spectrum corresponds to the reactant, and the maximum at 395 nm in the final spectrum, to the Fe(III) product. The main absorptions at ca. 400 nm in the first two spectra correspond to $[Fe(CN)_5NH_3]^{3-}$, which is present in equilibrium at pH 9.3. Time elapsed between initial and final spectra at both pH's, ca. 1 h.

the mixed-valent $[(NC)_5Fe^{III}NCFe^{II}(CN)_4H_2O]^{5-}$ ion.[31] This absorption disappears with initial 10^{-5} M $[Fe^{II}(CN)_5H_2O]^{3-}$, but the 395-nm absorption remains (bridge cleavage is achieved upon dilution, with persistence of the Fe(III)-chromophore in the mononuclear ion).[18] The inset in Figure 4 shows similar, slower changes observed at pH 9.3. In complementary experiments at pH's 7 and 9.3, oxygen was allowed to mix with $[Fe^{II}(CN)_5H_2O]^{3-}$ under the same conditions as with NH_2OH; remarkably equal final spectra were obtained, as shown in Figure SI 2. The product of reaction with O_2 has been early identified as $[Fe^{III}(CN)_5H_2O]^{2-}$.[18] To confirm the oxidation state of the metal, we added hydrazine to the mixed $[Fe(CN)_5H_2O]^{3-}-NH_2OH$ solution. Figure SI 3 shows a fast conversion of the 395-nm band into a new one centered at 440 nm ($\epsilon > 4500$ M^{-1} cm^{-1}), which further evolves slowly to a red complex absorbing at 520 nm ($\epsilon > 5500$ M^{-1} cm^{-1}). Along with the above changes, the decay of the NIR absorption is observed at the earliest stages. The experiments with hydrazine are quite relevant to the present study. As discussed below, the spectral changes associated with the 440 → 520-nm conversions also appear as main features of the NH_2OH-disproportionation reactions, although without the specific addition of hydrazine. Overall, the results show that the $[Fe(CN)_5H_2O]^{3-}-NH_2OH$ solutions display oxidizing activity, as expected for Fe(III) species reacting with hydrazine.[28] The similar, slower changes at pH 9.3 confirm that oxidation of the metal center occurs at all the studied pH's. The slow decay of the 395-nm absorptions with addition of a slight excess of NH_2OH suggests that a reductive fate of the Fe(III) species is operative.

The influence of the concentration of $[Fe(CN)_5H_2O]^{3-}$ on the spectroscopic observations was investigated in the range (2−6) $\times 10^{-3}$ M, still maintaining $R_0 < 1$, pH 7. The spectra of the solutions appear quite different, yielding equilibrium mixtures of the $[Fe(CN)_5H_2O]^{3-}$ ion and the cyano-bridged dimer $\{[Fe(CN)_5]_2H_2O\}^{6-}$ ($\lambda_{max} = 385$ nm).[31] However, the changes observed during the reaction with NH_2OH are similar to those at the lowest concentrations. We observe the increase of the product absorbance at ca. 385 nm and, again, a pronounced bending in the baseline for wavelengths above 700 nm. In other experiments with (2−6) $\times 10^{-3}$ M $[Fe(CN)_5H_2O]^{3-}$, $R_0 < 1$ and pH 7, we observe the evolution of N_2 but not of N_2O. In the exhausted solutions ammonia and NP are also found. This shows that, even under addition of substoichiometric initial NH_2OH, not only coordination and reduction but also oxidation ensues.

(v) Evidence for the Formation of NH_2 Radicals. When the reaction of NH_2OH with $[Fe(CN)_5NH_3]^{3-}$ is initiated in the presence of 0.1 M methyl methacrylate, we observed the development of a filamentous suspension, indicative of a radical-induced polymerization.[32] This was not observed in control experiments at pH 7−8 with aerated solutions of $[Fe(CN)_5NH_3]^{3-}$ in the absence of NH_2OH or with aerated solutions of NH_2OH in the absence of $[Fe(CN)_5NH_3]^{3-}$ Assuming a reductive cleavage of the N−O bond in NH_2OH, both amino (NH_2) or hydroxyl (OH) radicals could be formed. Each of them shows a different reactivity toward benzene.[33] NH_2 does not react with benzene under our reaction conditions, but the OH radical should react in a fast way yielding phenol. When the reactions were performed adding 20 mM benzene, no production of phenol was observed. Finally, a control experiment was made by mixing equimolar solutions of $[Fe(CN)_6]^{4-}$ with NH_2OH. No radicals were detected, and no spectral changes occurred, showing no reaction at all.

(31) (a) Emschwiller, G. *C. R. Acad. Sci. Paris* **1967**, *265*, 281−284. (b) Emschwiller, G.; Jorgensen, C. K. *Chem. Phys. Lett.* **1970**, *5*, 561−563. (c) Souto, M. F.; Cukiernik, F. D.; Forlano, P.; Olabe, J. A. *J. Coord. Chem.* **2001**, *54*, 343−353.

(32) (a) Kochi, J. K. *Free Radicals*; Wiley: 1973; Vol. II. (b) Corvaja, C.; Fischer, H.; Giacometti, G. *Z. Physik. Chem. Neue Folge* **1965**, *45*, 1−19.

(33) Neta, P.; Maruthamuthu, P.; Carton, P. M.; Fessenden, R. W. *J. Phys. Chem.* **1978**, *82*, 1875−1878.

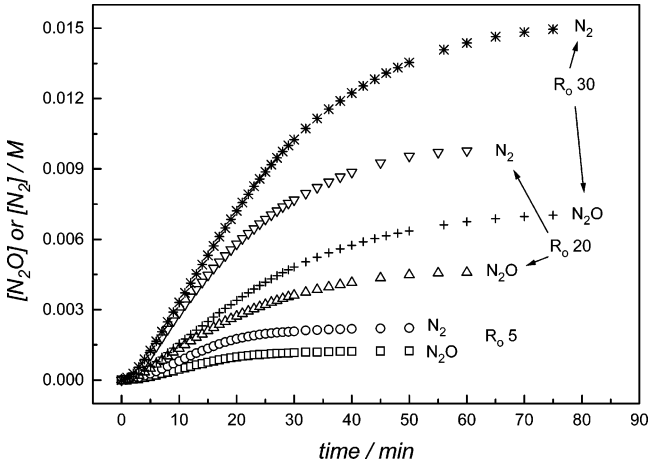

Figure 5. Time evolution of the gaseous products observed for the reaction between 2.5×10^{-3} M $[Fe(CN)_5H_2O]^{3-}$ and NH_2OH: 1.25×10^{-2} M, $R_0 = 5$, N_2O (□) N_2 (○); 5.0×10^{-2} M, $R_0 = 20$, N_2O (△) N_2 (▽); 7.5×10^{-2} M, $R_0 = 30$, N_2O (+) N_2 (∗); pH 7, $I = 1.9$ M (phosphates), $T = 25$ °C. Each curve reflects the accumulation of species in the reactor.

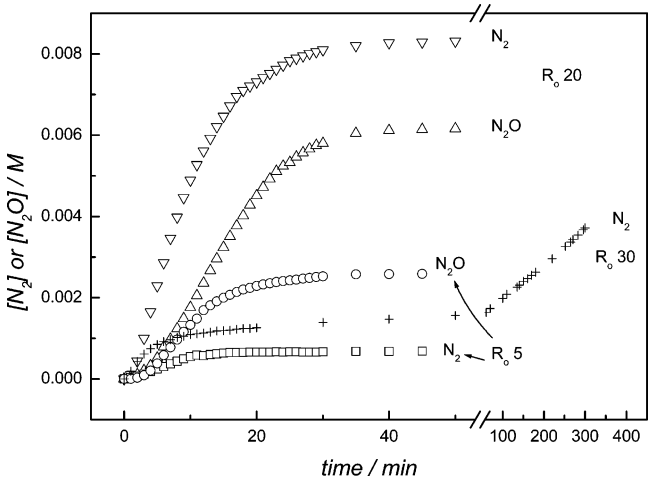

Figure 6. Time evolution of the gaseous products observed for the reaction between 2.5×10^{-3} M $[Fe(CN)_5H_2O]^{3-}$ and NH_2OH: 1.25×10^{-2} M, $R_0 = 5$, N_2O (○) N_2 (□); 5.0×10^{-2} M, $R_0 = 20$, N_2O (△) N_2 (▽); 7.5×10^{-2} M, $R_0 = 30$, N_2 (+); pH 9.3, $I = 0.2$ M (borates), 25 °C. For $R_0 = 30$, N_2 and N_2O are detected at the beginning, up to the plateau region.

(vi) Influence of pH and Concentration of NH_2OH in the Distribution of Gaseous Products. Table 1 displays the measured concentrations of N_2O and N_2 obtained in experiments with different initial concentration ratios of NH_2OH/complex (R_0) at different pH's. For nearly fixed concentrations of Fe(II) complex, the time elapsed for the complete transformation of increasing amounts of NH_2OH (between 0.0125 and 0.2 M) is approximately constant, ca. 50 min.

Figure 5 shows the S-shaped concentration−time profiles for the production of $[N_2]$ and $[N_2O]$ at pH 7.0. Remarkably, the N_2/N_2O ratios are close to 2 in most of the experiments (also at pH 6, Figure SI 4), with the only exception at a very high value of R_0, 85. At pH 8, Table 1 shows that more N_2O is produced for $R_0 = 2$, but the yield of N_2 increases gradually for greater R_0's (range 5−30; cf. also Figure SI 5 for pH 8, with a similar shape of the curves compared to those in Figure 5). The time needed to finish the process is now ca. 40 min, which is slightly smaller than the above-reported value in Figure 5. Figure 6 shows the corresponding changes in $[N_2O]$ and $[N_2]$ with time at pH 9.3. It shows a similar timing for the induction process

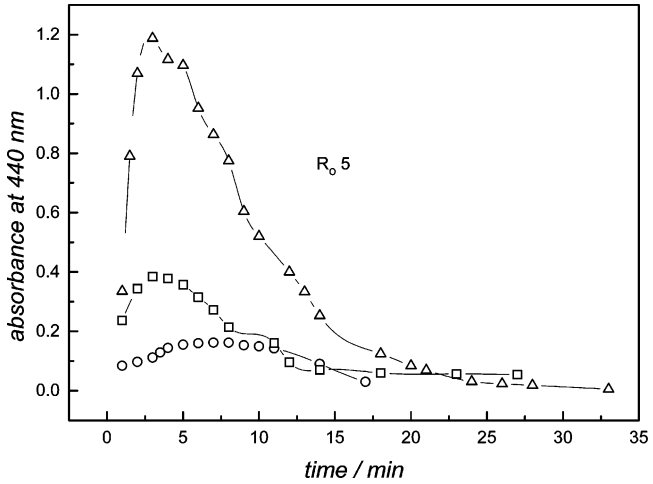

Figure 7. Absorbance at 440 nm vs time measured for the reaction between 2.5×10^{-3} M $[Fe(CN)_5H_2O]^{3-}$ and 1.25×10^{-2} M NH_2OH, $R_0 = 5$; (○) pH 7, (□) pH 8, (△) pH 9.3. $T = 25$ °C.

and also a similar dependence of the production of N_2 and N_2O with R_0 as described for pH 8. The time elapsed for reaching the plateau region is again shorter than for pH' s 7 and 8, ca. 30 min. This behavior, comprising the onset of a fast regime, shows that the rate increases with pH, although we do not observe proportional changes with the concentration of H^+.

At pH 9.3, we detect a new situation for $R_0 = 30$, not shown in the previous figures for lower pH's. At the early stages N_2, N_2O, and NH_3 were produced (rising part for the first 10 min), but when the transformed NH_2OH was around 10%, the reaction rate diminished noticeably. After this point, *only N_2 and NH_3* are produced, and this slow regime persists until completion. Turning back to Table 1, it can be seen that nearly exclusive yields of N_2 were also attained at $R_0 = 85$ and 40 for the lower pH' s 7 and 8, respectively (not shown in Figures 5 and SI 3). These values indicate that the change of regime occurs at any pH and is poorly sensitive to the concentration of NH_2OH. Further on, we will refer to the latter behavior as the *inhibited regime*.

In most of the above experiments, we observed that NP is also produced, with a pH-dependent final concentration. At pH 7, nearly 50% of the initial complex was transformed into NP. This fraction became smaller, down to 30% and 10% at pH's 8.0 and 9.3, respectively. However, NP was not found under the inhibited regime.

It is useful to compare the above results with the parallel changes in the intense 440-nm absorption band in experiments at ca. 10^{-3} M $[Fe(CN)_5H_2O]^{3-}$. Figure 7 shows the absorbance curves against time for $R_0 = 5$, at different pH's.

The rates of development of the band and the maximum attained intensity increase with pH. In all cases, the decay is fast and complete in 30 min. Note that the experiment at pH 7 reveals only a modest absorption. Figure 7 clearly shows the intermediate character of the 440-nm absorbing species in the *fast regime*, which evolves along with the production of N_2, N_2O, NP, and NH_3. In addition, a correlation was observed between the absorbance at 440 nm and the increase in the production of N_2, when the concentration of NH_2OH was increased at constant pH and complex concentration. Figure 8 shows the time evolution of the absorbance traces at 440 and 520 nm, for $R_0 = 30$, pH 9.3.

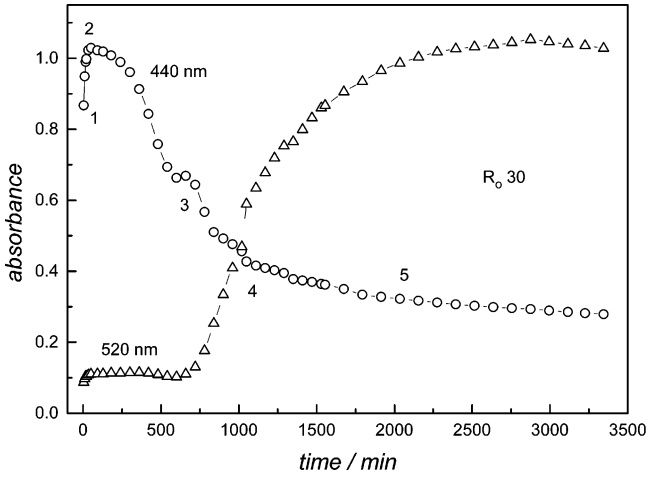

Figure 8. Absorbance vs time measured for the reaction between 2.5×10^{-3} M $[Fe(CN)_5H_2O]^{3-}$ and 7.5×10^{-2} M NH_2OH, ($R_0 = 30$); (○) 440 nm and (△) 520 nm; pH 9.3, $I = 0.2$ M (borates), $T = 25$ °C. (1) Fast absorbance increase for the first 10−15 min (corresponds to the initial fast production of N_2 and N_2O in Figure 6 for the same period). (2) Slowly decreasing plateau at 440 nm (corresponds to a constant rate of only N_2 production, up to 300−400 min; note the change in scale in Figure 6. (3) For $t = 600$ min the 520-nm band emerges and the rate of N_2 production increases (not seen in Figure 6). (4) Up to 1000 min, $A_{440} = A_{520}$, and the consumption of NH_2OH is ca. 50%. The rate of N_2 production still increases. (5) The production of N_2 drops abruptly. Maximum intensity of the 520-nm band. Total consumption of NH_2OH.

Note that the conditions correspond to the *inhibited regime* (cf. Figure 6). The buildup of the 440-nm band, rapidly attaining high intensity, is followed by a very slow decay, compared with the one observed for $R_0 = 5$ in Figure 7 at the same pH.[34] It is instructive to compare the absorbance values in Figure 8 with the gas production measurements in Figure 6 (same conditions, $R_0 = 30$), along with the degree of consumption of NH_2OH. We describe in the legend of Figure 8 the different time-dependent features of these indicators. Both species were very light-sensitive, although stable in the darkness. When the measurements were performed under illumination, the N_2 production behavior was similar, but the 520-nm band intensity was smaller and decayed down to zero along with the stop in the production of N_2. Finally, the 440−520-nm conversions were also detectable under the *fast regime* conditions, where the 520-nm absorptions behaved as transients, along with the 440-nm decays.

(vii) Characterization of Intermediates in the Solutions with an Intense 440 nm Absorption. (a) Resonance Raman. Figure 9 shows the spectrum in aqueous solution, after irradiation close to the maximum of the long-lived 440-nm band. The main absorption appears at 1482 cm^{-1}, together with several peaks in the range 2060−2100 cm^{-1}, which are typical of cyanide-stretching vibrations associated with Fe(II).[13] Absorptions at 1639, 1556, 989, and 917 cm^{-1} correspond to buffer components. The peak at 1482 cm^{-1} can be assigned to the N═N stretching, by comparison with absorptions measured in other diazene complexes.[35a] Stronger and conclusive evidence on diazene coordination is given by the downward shift of the latter absorption to 1438 cm^{-1}, when initial $^{15}NH_2OH$ was used. This is in full agreement with a doubly labeled ^{15}N-species.[35a]

(b) UV−vis. The estimation of the molar absorbance, $\epsilon \geq 4500$ M^{-1} cm^{-1} was done under conditions favoring the fast formation of the intermediate (cf. Figure 8). The absorption properties are consistent with similar features found in diazene complexes.[35b]

(c) ^{15}N NMR. Figure 10 shows the spectrum of a reaction mixture of excess $^{15}NH_2OH$ with $[Fe(CN)_5NH_3]^{3-}$ at pH ≈ 9 containing the long-lived 440-nm absorption band. Five signals are observed at −76, −242, −281, −339 and −373 ppm, relative to CH_3NO_2 as external standard.[36] The most intense one at −281 ppm is presently assigned to free NH_2OH, while the other are in principle assigned to species arising as steady-state intermediates. The peaks at −372 and −339 ppm can be traced to NH_3 and N_2H_4, respectively (the latter one could also correspond to a structurally related intermediate), and the very weak one at −242 ppm could be due to bound NH_2OH.[37] Finally, the last signal at −76 ppm can be confidently assigned to the bound diazene intermediate.[37] This last compound is expected to generate two different signals for each nitrogen atom, unless HN═NH is coordinated in an η^2 mode or there is a fluxional coordination exchange between both nitrogen atoms.

(d) Chemical Evidence. The 440 → 520-nm conversion in Figure 8 is clearly indicative of a mononuclear → dinuclear transformation involving bridged diazene. The same process has been found with hydrazine as a precursor, in oxidizing conditions (see also Experimental Section and Results, section iv).[28]

(e) Competitive Experiments. For $R_0 > 40$, at 25.0 °C and pH 8−9.3, with the reactions operating under the *inhibited regime* (persistence of the 440-nm absorption), we observed that the reduction of ethylene to ethane competes with the disproportionation of NH_2OH to N_2 and NH_3. In this situation we did not observe the development of the band centered at 520 nm. These hydrogenation processes are typical of diazene reactivity.[38]

Discussion

The reaction of NH_2OH with cyanoferrates appears quite complex. Large quantities of NH_2OH are consumed by starting with $[Fe^{II}(CN)_5H_2O]^{3-}$ leading to reduction (NH_3) and oxidation (N_2, N_2O, NO^+) products, with the participation of free radicals. The appearance of N_2H_2 as a bound intermediate is unprecedented in previous studies of NH_2OH redox chemistry. The time evolution and the dependence on pH, as well as on the NH_2OH concentration for the formation of products, place a high premium on understanding the mechanism of the disproportionation process. We anticipate a simplified Scheme 1, consistent with the known chemistry of the reactive species involved, followed by a more detailed description of the proposed paths.

We analyze first the conditions chosen to handle the solutions. For the $[Fe^{II}(CN)_5L]^{3-}$ complexes (L = H_2O, NH_3, NH_2OH,

(34) The high intensity and slow decay of the 440-nm band are observed at other R_0 values for different initial concentrations of $[Fe(CN)_5H_2O]^{3-}$. Thus, at pH 7 and $(1-2) \times 10^{-5}$ M $[Fe(CN)_5H_2O]^{3-}$, it was observed for R_0 ca. 5−6.

(35) (a) Lehnert, N.; Wiesler, B. E.; Tuczek, F.; Hennige, A.; Sellmann, D. *J. Am. Chem. Soc.* **1997**, *119*, 8879−8888. (b) *ibid.* **1997**, *119*, 8869−8878.

(36) The proton-decoupled ^{15}N NMR spectrum has an inherent low sensitivity, nearly an order of magnitude less than ^{13}C signals. Unfavorable sensitivity conditions in our system are given by the dynamic evolution and bubble formation. Routine measurements with ^{15}N NMR usually require concentrations in the range 100−1000 mM, which are nearly an order of magnitude greater than those used in the present study (cf. Silverstein, R. M.; Webster, F. X. *Spectrometric Identification of Organic Compounds*, 6th ed.; Wiley: 1997).

(37) Mason, J. *Chem. Rev.* **1981**, *81*, 205−227.

(38) (a) Stanbury, D. M. *Prog. Inorg. Chem.* **1998**, *47*, 511−561. (b) Back, R. A. *Rev. Chem. Intermed.* **1984**, *5*, 293−323. (c) Hunig, S.; Muller, H. R.; Thier, W. *Tetrahedron Lett.* **1961**, *11*, 353−357.

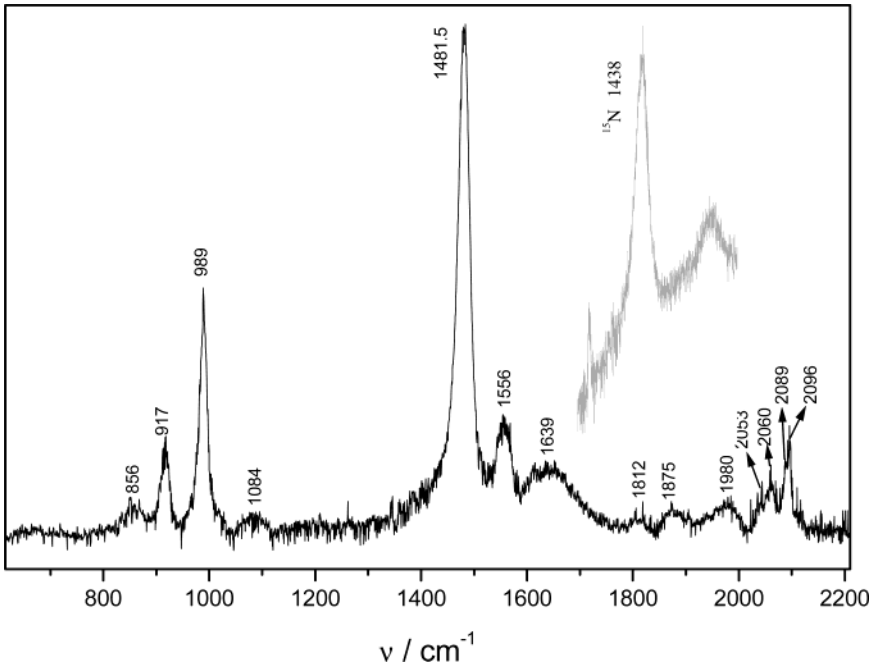

Figure 9. Resonance Raman spectrum of the solution containing the 440-nm long-lived species. See Experimental Section for the measurement conditions. The peak at upper-right corresponds to the most intense absorption in a complementary experiment with initially labeled hydroxylamine (^{15}N).

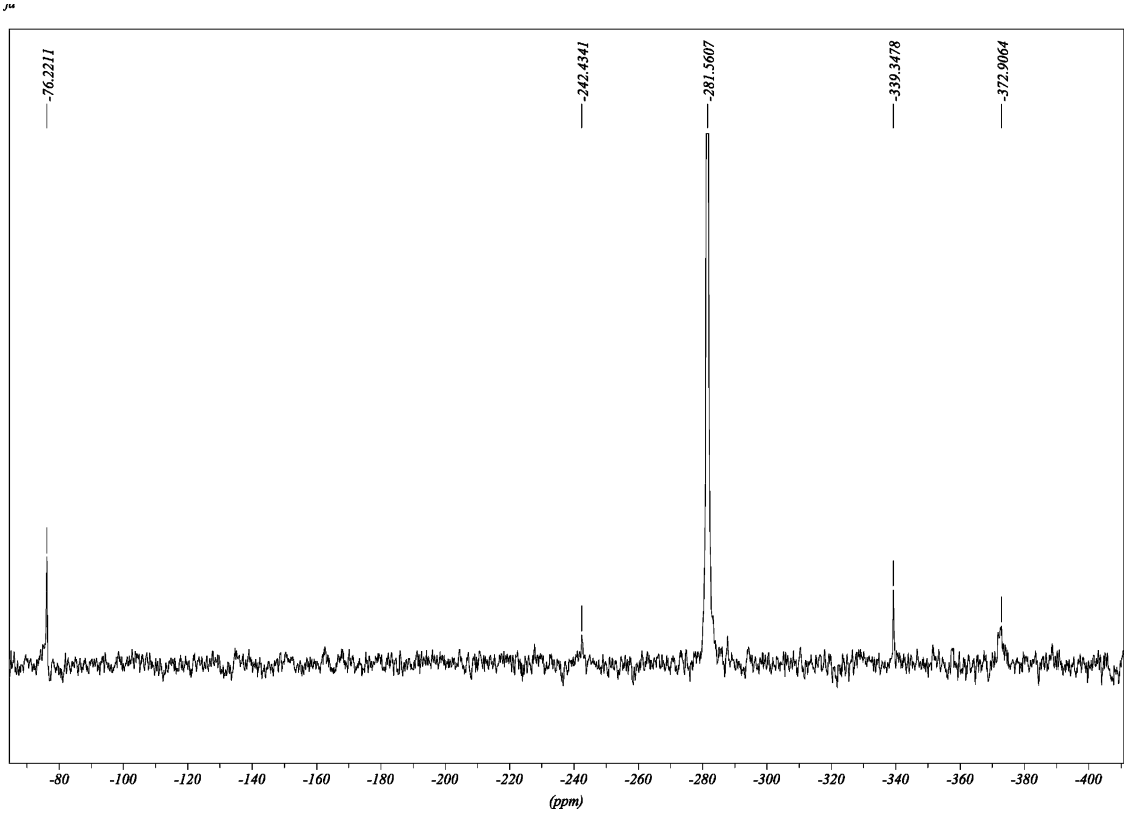

Figure 10. ^{15}N NMR spectrum of the solution containing the long-lived 440-nm absorbing species. See Experimental Section for the measurement conditions.

N_2H_4, N_2H_2, etc.), full cyanide deprotonation is ensured at pH 6.0, the lowest used in the experiments.[39] The relevant pK_a's for NH_3OH^+ and NH_2OH are 5.9 and 13.7, respectively.[8] These values could be decreased by ca. 2 pK_a units upon coordination.[29] We conclude that NH_2OH should be the predominant species in our reaction conditions. For the possible oxidized intermediates $[Fe^{III}(CN)_5L]^{2-}$, deprotonation of L may occur significantly at pH's greater than 8.[40] Upon dissolution of solid $Na_3[Fe^{II}(CN)_5NH_3]\cdot 3H_2O$, reaction 1 is onset:

$$[Fe^{II}(CN)_5NH_3]^{3-} + H_2O \rightleftharpoons [Fe^{II}(CN)_5H_2O]^{3-} + NH_3 \quad (1)$$

The values of k_1 and k_{-1} are 1.75×10^{-2} s^{-1} and 365 M^{-1} s^{-1}, respectively (25.0 °C, $I = 0.1$ M).[41] The pH range 6−8 is

(39) (a) Toma, H. E.; Malin, J. M. *Inorg. Chem.* **1973**, *12*, 1039−1045. (b) Malin, J. M.; Koch, R. C. *Inorg. Chem.* **1978**, *17*, 752−754.

Scheme 1

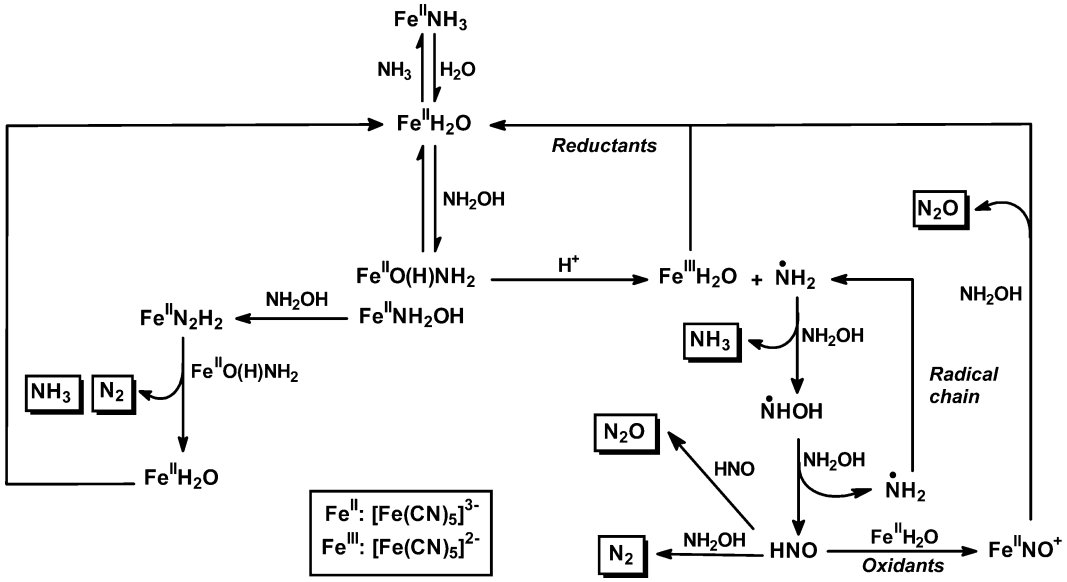

sufficiently low for trapping most of the produced NH_3 as NH_4^+ (pK_a 9.24),[42] thus allowing for the regeneration of $[Fe^{II}(CN)_5H_2O]^{3-}$ in the reaction medium.

Spectral and kinetic evidence on the coordination of NH_2OH have been presented. The second-order rate constant in Figure 3 is consistent with similar values found for the coordination of neutral ligands into $[Fe^{II}(CN)_5H_2O]^{3-}$, such as NH_3 (see eq 1), amines, N_2H_4, etc..[13,41]

The initial wavelength shift in Figure 2 can be interpreted through reactions 2a and 2b, considering two alternative coordination modes of NH_2OH.[8,13]

$$[Fe^{II}(CN)_5H_2O]^{3-} + NH_2OH \rightleftharpoons [Fe^{II}(CN)_5O(H)NH_2]^{3-} + H_2O \quad (2a)$$

$$[Fe^{II}(CN)_5H_2O]^{3-} + NH_2OH \rightleftharpoons [Fe^{II}(CN)_5NH_2OH]^{3-} + H_2O \quad (2b)$$

The evidence on the Fe(III) oxidized product and radical formation implies that a follow-up to coordination must occur. We propose reaction 3:

$$[Fe^{II}(CN)_5O(H)NH_2]^{3-} + H^+ \rightarrow [Fe^{III}(CN)_5H_2O]^{2-} + NH_2 \quad (3)$$

The primary interaction described by eqs 2−3 agrees with the slower oxidation observed with increasing pH. This picture is in contrast with the lack of substitutional or redox reactivity of $[Fe^{II}(CN)_6]^{4-}$ toward NH_2OH. As the redox potentials of hexa- and pentacyano-complexes are similar (ca. 0.4 V),[13] it becomes evident that iron-oxidation requires an inner-sphere path.

The Fe(III) ion generated in reaction 3 goes back to Fe(II) under reductive conditions, mainly provided by the excess NH_2OH.[20] On the other hand, the production and role of the oxidizing NH_2 radicals[43] in the reduction of NH_2OH by transition metal complexes has been previously documented.[8] In the Results section, we emphasized on a reaction process that switched between a fast and a slow, inhibited regime. We interpret it as the reaction following at least two different pathways. One produces a certain intermediate, while another one consumes it. Then, the intermediate concentration functions as a trigger for the change of regime. For high concentrations the reaction attains the *fast regime*. Eventually the intermediate concentration may be decreased enough, shifting the reaction path to the slow, *inhibited regime*. As anticipated in Scheme 1, we consider the NH_2 radical as the active intermediate. Then, reaction 3 is the initiation of a chain reaction, with reactions 4 and 5 operating as propagation steps.

$$NH_2 + NH_2OH \rightarrow NH_3 + NHOH \quad (4)$$

$$NHOH + NH_2OH \rightarrow HNO + H_2O + NH_2 \quad (5)$$

Reactions 4 and 5 are thermodynamically allowed in our reaction conditions.[43,44] The observed induction period (see Figures 5, 6, SI 4, and SI 5) is also indicative of this complex kinetics.[45] According to our simulations, the induction is controlled by the slow reactions 3 and 5. Thus, the basis is set for the fast catalytic consumption of NH_2OH through the formation of oxidized and reduced products. HNO (nitroxyl)[46] appears as a plausible intermediate in our reaction conditions,

(40) (a) Davies, G.; Garafalo, A. R. *Inorg. Chim. Acta* **1976**, *19*, L3−L4. (b) Davies, G.; Garafalo, A. R. *Inorg. Chem.* **1976**, *15*, 1101−1106.
(41) Toma, H. E.; Batista, A. A.; Gray, H. B. *J. Am. Chem. Soc.* **1982**, *104*, 7509−7515. The formation rate constants for the coordination of neutral ligands into $[Fe(CN)_5H_2O]^{3-}$ decrease slightly with the ionic strength, with reported values of ca. 2×10^2 M^{-1} s^{-1} at $I = 1$ M.
(42) Fasman, G. D. *Handbook of Biochemistry and Molecular Biology, Physical and Chemical Data*; CRC Press: Cleveland, OH, 1976; Vol. 1.
(43) Stanbury, D. M. *Adv. Inorg. Chem.* **1989**, *33*, 69−138.
(44) Free energies for reactions 4 and 5 were calculated as −106 kJ mol^{-1} and −0.8 kJ mol^{-1}, respectively. The chain propagation and its precursor, reaction 3, reveal a close analogy between hydroxylamine and hydrogen peroxide chemistry (Fenton-type), with Fe(II) species leading to free radicals (cf. Jones, C. W. *Applications of Hydrogen Peroxide and Derivatives*; The Royal Society of Chemistry: U.K., 1999; p 44).
(45) Benson, S. W. *Foundations of Chemical Kinetics;* McGraw-Hill Book Co.: New York, 1960.

a precursor of N_2O and N_2 according to the fast reactions 6 and 7:[8]

$$2HNO \rightarrow N_2O + H_2O \quad (6)$$

$$HNO + NH_2OH \rightarrow N_2 + 2H_2O \quad (7)$$

The set of reactions 4−7 sustain the NH_2OH processing and agree with the stoichiometry found in the *fast regime* conditions. The relative enrichment of N_2 with an increasing concentration of initial NH_2OH is consistent with reaction 7 being favored over reaction 6 (cf. Table 1). The production of N_2O could only be realized for R_0's > 1. No production was observed upon treatment with substoichiometric NH_2OH, given that NP and N_2 did form, and this can be traced to the rapid depletion of NH_2OH.

In parallel with the *radical path*, the formation and decay of the 440-nm band has been observed (Figures 2 and 7). We have already identified the species absorbing at this wavelength as $[Fe^{II}(CN)_5N_2H_2]^{3-}$, and we propose that it is formed through reaction 8:

$$[Fe^{II}(CN)_5NH_2OH]^{3-} + NH_2OH \rightarrow [Fe^{II}(CN)_5N_2H_2]^{3-} + 2H_2O \quad (8)$$

The 440-nm band was previously traced to the $[Fe^{II}(CN)_5NH_2OH]^{3-}$ complex.[12,15,49] However, the *d*−*d* transitions in $[Fe^{II}(CN)_5L]^{3-}$ complexes with L = *N*-binding saturated ligands, NH_3, amines and diamines, N_2H_4, appear all around 400 nm, with ϵ = ca. 500 M^{-1} cm^{-1}.[13] The intense 440-nm band can be more reasonably assigned to a metal-to-ligand charge-transfer (MLCT) transition from Fe(II) to the vacant π^* orbital in the $[Fe^{II}(CN)_5N_2H_2]^{3-}$ ion.[35b] There are several examples of well characterized monodentate coordination of N_2H_2 in low-spin d^6 complexes.[50] The $[Fe^{II}(CN)_5N_2H_2]^{3-}$ ion must be moderately inert toward dissociation of N_2H_2, according to its $\sigma-\pi$ bonding properties,[35] but it should be destroyed by the oxidants existing in the reaction pool.

The termination reactions for the NH_2 radical can be envisaged through a secondary interaction with $[Fe^{II}(CN)_5L]^{3-}$ reductants (L = H_2O, N_2H_2, etc.) or through the less probable (in most of our experimental conditions) self-reaction giving hydrazine.[47]

Equation 8 describes a competitive reaction, regarding eq 3, for the decay of $[Fe^{II}(CN)_5O(H)NH_2]^{3-}$,[48] and it becomes predominant with increasing pH's and NH_2OH-concentration. The $[Fe^{II}(CN)_5N_2H_2]^{3-}$ ion traps most of the iron sites, the NH_2 radical concentration has been sufficiently depleted through the termination steps, and the reaction develops very slowly (see Figure 6). In these conditions, bound diazene decays mainly through reaction 9.[38,51]

$$[Fe^{II}(CN)_5N_2H_2]^{3-} + [Fe^{II}(CN)_5O(H)NH_2]^{3-} \rightarrow 2\,[Fe^{II}(CN)_5H_2O]^{3-} + N_2 + NH_3 \quad (9)$$

Reactions 8 and 9 satisfy the equimolar stoichiometry found for the N_2 and NH_3 production in the *inhibited regime* and also sustain the slow molecular path for NH_2OH processing anticipated in the scheme.

Figure 8 indicates that after the slowly decreasing plateau corresponding to the inhibited regime, the $[Fe^{II}(CN)_5N_2H_2]^{3-}$ ion becomes the precursor of a species absorbing at 520 nm, which we already assigned to the bridged-diazene dimer. Its RR spectrum showed a band at 1440 cm^{-1} after irradiation at 515 nm,[28] and this frequency is consistently lower than the one assigned above to $[Fe^{II}(CN)_5N_2H_2]^{3-}$. Therefore, we propose reaction 10, consistent with a specific test described in the Experimental Section:

$$[Fe^{II}(CN)_5N_2H_2]^{3-} + [Fe^{II}(CN)_5H_2O]^{3-} \rightleftharpoons [(NC)_5Fe^{II}HN{=}NHFe^{II}(CN)_5]^{6-} + H_2O \quad (10)$$

The dimer is quite stable although light sensitive and decomposes giving N_2 if oxygen or other oxidants are present. The appearance of the dimer goes in parallel with a faster evolution of N_2 (see legend in Figure 8). This can be explained because more $[Fe^{II}(CN)_5H_2O]^{3-}$ and oxidant are available as far as NH_2OH is being consumed. The $[Fe^{II}(CN)_5H_2O]^{3-}$ ion binds competitively to the $[Fe^{II}(CN)_5N_2H_2]^{3-}$ complex and simultaneously promotes more NH_2OH decomposition (through reaction 2a) and subsequent N_2 production.

To explain fully the diversified product pattern, we come again to the radical path. As well as leading to N_2 and N_2O production, HNO can be oxidized to NO^+. The identification of NP as an oxidation product at an early stage of the process provides complementary evidence of the formation of HNO[46] in the propagation chain. The possibility of obtaining NP from NH_2OH has been anticipated.[52] Successive two-electron processes have been proposed for the oxidation by high-valent aqueous metal ions[8,53] and in the enzymatic HAO-mediated conversions of NH_2OH to nitrite.[4] Good stoichiometric evidence has been found for the participation of $[Fe^{II}(CN)_5HNO]^{3-}$ in the full six-electron reduction of NP to NH_3.[26] Theoretical calculations have been reported providing evidence on the stability, geometry, and spectroscopy of $[Fe^{II}(CN)_5HNO]^{3-}$.[54]

(46) (a) Bonner, F. T.; Dzelzkalns, L. S.; Bonucci, J. A. *Inorg. Chem.* **1978**, *17*, 2487−2494. (b) Akhtar, M. J.; Bonner, F. T.; Borer, A.; Cooke, I.; Hughes, M. N. *Inorg. Chem.* **1987**, *26*, 4379−4382. (c) Southern, J. S.; Hillhouse, G. L. *J. Am. Chem. Soc.* **1997**, *119*, 12406−12407. (d) Bartberger, M. D.; Fukuto, J. M.; Houk, K. N. *Proc. Natl. Acad. Sci. U.S.A.* **2001**, *98*, 2194−2198. (e) Shafirovich, V.; Lymar, S. V. *Proc. Natl. Acad. Sci. U.S.A.* **2002**, *99*, 7340−7345. (f) Sulc, F.; Immoos, C. E.; Pervitsky, D.; Farmer, P. J. *J. Am. Chem. Soc.* **2004**, *126*, 1096−1101.

(47) Laszlo, B.; Alfassi, Z. B.; Neta, P.; Huie, R. E. *J. Phys. Chem. A* **1998**, *102*, 8498−8504.

(48) Equation 8 comprises a condensation process for NH_2OH, with possible unknown intermediate formation. In eq 8, the competition with reaction 3 could be better appreciated if the O-bound complex would be the reactant. However, the N-bound complex was considered a more realistic approach to diazene formation, given that the competition with reaction 3 is still established through reactions 2a and b.

(49) Mulvey, D.; Waters, W. A. *J. Chem. Soc., Dalton Trans.* **1975**, 951−959.

(50) (a) Smith, M. R., III; Cheng, T. Y.; Hillhouse, G. L. *J. Am. Chem. Soc.* **1993**, *115*, 8638−8642. (b) Cheng, T. Y.; Ponce, A.; Rheingold, A. L.; Hillhouse, G. L. *Angew. Chem., Int. Ed. Engl.* **1994**, *33*, 657−659. (c) Marchenko, A. V.; Vedernikow, A. N.; Dye, D. F.; Pink, M.; Zaleski, J. M.; Caulton, K. G. *Inorg. Chem.* **2004**, *43*, 351−360.

(51) Equation 9 has been written after calculating that the one-electron outer sphere oxidation of $[Fe^{II}(CN)_5N_2H_2]^{3-}$ by free NH_2OH is endergonic. The one-electron reduction potential for the couple NH_2OH/NH_2, OH^- is −0.6 V, estimated considering the following ΔG^0_f values: −23.4, 192, and −157.8 kJ mol^{-1} for NH_2OH, NH_2 radical, and OH^- ion in aqueous solution, respectively. The potential for the $[Fe^{III,II}(CN)_5N_2H_2]^{2-,3-}$ couple should be of ca. 0.5 V.[13]

(52) Caulton, K. G. *Coord. Chem. Rev.* **1975**, *14*, 317−355.

(53) Johnson, M. D.; Hornstein, B. J. *Inorg. Chem.* **2003**, *42*, 6923−6928.

(54) González Lebrero, M. C.; Scherlis, D. A.; Estiú, G. L.; Olabe, J. A.; Estrin, D. A. *Inorg. Chem.* **2001**, *40*, 4127−4133.

The decreasing yield of NP in the exhausted solutions for increasing pH's can be traced to the incidence of the well-established reaction of NP with NH_2OH.[16]

$$[Fe^{II}(CN)_5NO]^{2-} + NH_2OH + OH^- \rightarrow [Fe^{II}(CN)_5H_2O]^{3-} + N_2O + H_2O \quad (11)$$

Our previous analysis has been done considering mononuclear complexes, although equilibrium mixtures of $[Fe^{II}(CN)_5H_2O]^{3-}$ and $[(NC)_5Fe^{II}NCFe^{II}(CN)_4H_2O]^{6-}$ exist in the solutions under some of our experimental conditions.[31,55] The first ion predominates at ca. $(1-3) \times 10^{-5}$ M, with increasing amounts of the dimer for greater concentrations. In oxidative conditions and a low concentration of NH_2OH, mixed-valent dinuclear complexes are produced.[31] In excess of NH_2OH however the mixed valent complexes were not observed at all, suggesting a bridge cleavage and the predominance of mononuclear species. In either case, the coordination of substrates and subsequent reactions involving the labile iron-aqua site in the mixed-valent dimers should be similar to those proposed for the mononuclear ions.

Finally, we refer to the simulation results and interpretation. A simplified mechanism has been employed, emphasizing in the main oxidation and reduction products, with omission of the NP and bridged-diazene formation reactions. All the possible reactions presented explicitly or implicitly in the Discussion have been considered, as shown in Scheme SI 6, with the values of the rate constants extracted from the literature, as well as the ones which were considered as fitting parameters. We choosed pH 7 for the calculations, having in mind that the observed behavior was similar at the different pH's. Through this procedure, the importance and the relative sensibility of the reactions were studied, allowing for the establishment of a minimum scheme. The main focusing requirements deal with the induction periods, the distribution of products (N_2, N_2O, and NH_3) and the conditions for the change of regime. The output in Figures SI 7 and 8 reproduces qualitatively the most important focused points, namely the following: (a) At a constant iron concentration, different initial concentrations of NH_2OH (ca. 0.025 M to 0.2 M) are processed in approximately the same time period. (b) The distribution of gaseous products shows enrichment in N_2 with increasing concentration of initial NH_2OH, up to a critical value after which the production is much slower. (c) The global yield of NH_3 is well reproduced.[56]

Conclusions

NH_2OH transforms to NH_3 and diverse oxidation products (N_2, N_2O, NO^+) in different yields according to pH and concentration of initial substrate. With $[Fe^{II}(CN)_5NH_3]^{3-}$ as the initial precursor, great amounts of NH_2OH can be processed, with $[Fe^{II}(CN)_5H_2O]^{3-}$ as the cycling catalyst. Catalysis is inhibited by strongly binding ligands such as cyanide.

Coordination of NH_2OH to $[Fe^{II}(CN)_5H_2O]^{3-}$ and production of NH_2 sets the basis for establishing a fast *radical path* leading to reduced and oxidized products, NH_3 and nitroxyl, HNO, respectively. The latter species is the precursor for the formation of N_2 and N_2O and can be further oxidized to NP. A slow *molecular path*, accomplished simultaneously with the above-described one, is operative for high concentrations of NH_2OH. The NH_2 radical concentration becomes low and the $[Fe^{II}(CN)_5N_2H_2]^{3-}$ ion accumulates in the medium, trapping most of the iron sites. Thus, it can be characterized by chemical and spectroscopic tools (RR, UV−vis, ^{15}NMR). In certain conditions, the $[(NC)_5Fe^{II}HN{=}NHFe^{II}(CN)_5]^{6-}$ ion remains in the exhausted solutions after consumption of NH_2OH. The intermediacy of well characterized diazene complexes is a novel result in the redox chemistry of NH_2OH.

The production of minor quantities of NP compared to the other products leads to some resemblance with the behavior of the HAO enzyme. The formation of NP in our reaction conditions, although mechanistically quite significant, is not catalytic however for the production of nitrite. Moreover, given the strong $Fe-NO^+$ bond in NP, the catalytic iron site becomes partially blocked, because the NO^+/NO_2^- conversion and release of nitrite occur at pH's > 10. This is in contrast with HAO, which presumably releases nitrite at lower pH's, thus allowing for further coordination and processing of NH_2OH.

Acknowledgment. This work was supported by the Universities of Buenos Aires and Mar del Plata, the Government Agencies ANPCYT and CONICET, and by the Volkswagen-Stiftung (Germany). We appreciate the aid of Professor Daniel Murgida (University of Berlin) in performing the RR measurements and the collaboration of Dr. Alejandro R. Parise with some experiments. V.T.A., F.D., and J.A.O. are members of the scientific staff of CONICET.

Supporting Information Available: Figures: SI 1 (Logarithmic plots for the reaction of $[Fe^{II}(CN)_5H_2O]^{3-}$ with excess NH_2OH). SI 2 (Reaction of O_2 with $[Fe^{II}(CN)_5H_2O]^{3-}$, in similar conditions as with NH_2OH). SI 3 (Reaction of hydrazine with the reaction product of $[Fe^{II}(CN)_5H_2O]^{3-}$ and NH_2OH). SI 4 (Time evolution of gaseous products at pH 6). SI 5 (Time evolution of gaseous products at pH 8). Scheme SI 6 (List of reactions and associated rate constants employed in the simulations). Figures: SI 7 (Simulation of time evolution of the concentration of N_2 and N_2O at different values of R_0). SI 8 (Simulation of time evolution of the concentration of $[Fe^{II}(CN)_5N_2H_2]^{3-}$ at different values of R_0). This material is available free of charge via the Internet at http://pubs.acs.org.

JA046724I

(55) James, A. D.; Murray, R. S. *J. Chem. Soc., Dalton Trans.* **1977**, 326−329.
(56) Ongoing experiments aim to better explore the transition region through a broader variation of pH's and concentrations of hydroxylamine. These results will be reported in due course.